

Supporting Information

Encapsulating electron-deficient dyes into Metal-Organic Capsules To Achieve High Reduction Potentials

Contents

1. Experimental Section
2. Crystallography
3. ESI-MS Spectra data
4. Characterization of Host-Guest
5. Data for the photocatalytic reactions
6. References

1. Experimental Section.

Materials and methods

Unless otherwise stated, all chemicals were of reagent grade quality obtained from commercial sources and were used without further purification. Solvents to be dried were obtained by standard methods of drying and distillation.

^1H NMR spectra were measured on a Varian INOVA-400M spectrometer. The ESI mass spectra were performed on an HPLCQ-ToF MS spectrometer using methanol/acetonitrile as mobile phase. The elemental analyses of C, H and N were performed on a Vario EL III elemental analyzer. The isothermal titration calorimetry experiments were performed on a Nano ITC (TA Instruments Inc.–Waters LLC) at atmospheric parameters and at 25.0 °C, giving the association constants and the thermodynamic parameters. The solution fluorescent spectra were measured on Edinburgh FS-920 using 395 nm, the same wavelength as the LEDs light source, as the excitation wavelength. The UV-Vis spectra of solutions were measured on a SHIMADZU UV 2600 spectrophotometer. The light sources are 395 nm LEDs (30 W) were purchased from Shenzhen Xinxingyuan Photoelectric Technology. The photon power density is measured by CEL-NP2000-2A photoradiometer from CEALight Company Limited. All electrochemical measurements were performed on a CHI 660E electrochemical workstation with a three-electrode system, with Ag/AgCl electrode as reference electrode, platinum silk as counter electrode, and glassy carbon electrode as working electrode, and. The GC analysis was measured on a SHIMADZU GC-2014 instrument equipped with FID detector and HP-5 GC column (Agilent Technologies),

using N₂ as carrier gas.

Synthesis of Zn-PAP

N1,N1'-(1,4-Phenylene)bis-(N1-(4-aminophenyl)benzene-1,4-diamine) (47 mg, 0.1 mmol), 2-Pyridinecarboxaldehyde (45 μ L, 0.4 mmol), and Zn(ClO₄)₂ (52 mg, 0.14 mmol) were added to 30 mL dry acetonitrile solution. The solution was purged with argon three times and then reacted at 70 °C for 24 hours. The reaction solution was diffused in diethyl ether to obtain dark red crystals of Zn-PAP. Yield: 30%.

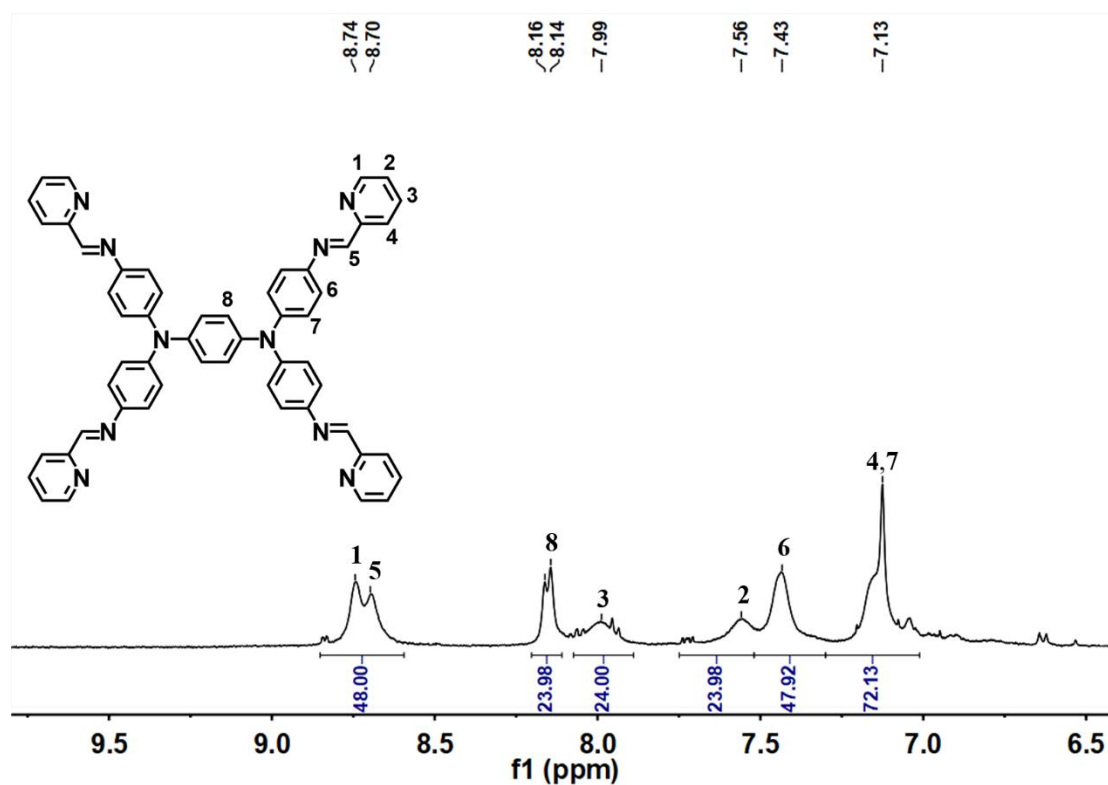


Figure S1. ¹H-NMR spectrum of Zn-PAP in d⁶-DMSO.

General procedure for catalytic reactions

All catalytic reactions were performed under 395 nm LED lights (30 W). The reaction temperature was maintained at room temperature by circulating water through the outer packaging of the reactor. The yields of the dechlorinated product were determined by

GC analysis on Shimadzu GC-2014 instrument equipped with FID detector and HP-5 GC column (Agilent Technologies), using N₂ as carrier gas. The standard catalytic reaction steps were as follows: substrates (50 μmol, 1 equiv), **Zn-PAP** (0.5 μmol, 1 mol%), **AQ** (0.5 μmol, 1 mol%), and Na₂CO₃ (30 μmol, 0.6 equiv) were dissolved in 3 mL DMAC to a 10 mL quartz Schlenk tube. The mixture was bubbled with argon for 10 minutes, then stirred and irradiated with an LED lights (2×30 W, 395 nm) for 30 minutes at room temperature (acetophenone as internal standard). Kinetic experiments of the Michaelis-Menten mechanism analysis were carried out under different conditions using 4-chlorobenzamide as the substrate. The yields of benzamide products in the initial reaction stages were regarded as the initial rate of the reactions.

2. Crystallography

Single crystal X-ray diffraction measurements of **Zn-PAP** were performed on a Bruker SMART APEX CCD diffractometer equipped with graphite monochromatic Mo K α ($\lambda = 0.71073 \text{ \AA}$) radiation at 120 K. The data were obtained using the SMART and SAINT programs.^{S1,S2} The structure was solved with the intrinsic fixed-phase method (SHELXT-2015) and refined by full-matrix least-squares on F^2 using the SHELXL-2015 module of OLEX2.^{S3,S4} All the non-hydrogen atoms were refined by full-matrix least-squares techniques with anisotropic displacement parameters. And the hydrogen atoms were geometrically fixed at the calculated positions attached to their parent atoms, treated as riding atoms. Due to the poor quality of the crystal data, SIMU, ISOR, and DFIX constraints were used to obtain reasonable parameters. Local occupancy of the main solvent peaks was localized and refined due to severe disorder caused by thermal motion or dynamic localization of solvent accessible space. Several bond distances in the counter ClO $_4^-$ ions were restrained as idealized values. The remaining unassigned electron densities were removed utilizing the SQUEEZE program implemented in PLATON.

Crystal data for **Zn-PAP**: C $_{342}$ H $_{263}$ Cl $_{16}$ N $_{66}$ O $_{64}$ Zn $_8$, Mr = 7411.33, Triclinic space group P-1, dark-red block, $a = 23.386(7) \text{ \AA}$, $b = 24.387(8) \text{ \AA}$, $c = 38.081(11) \text{ \AA}$, $\alpha = 97.486(7)$, $\beta = 95.237(7)$, $\gamma = 105.524(7)$, $V = 20565(11) \text{ \AA}^3$, $Z = 2$, Dc = 1.197 g cm $^{-3}$, T = 120(2) K, $\mu(\text{Mo-K}\alpha) = 0.634 \text{ mm}^{-1}$. [Rint = 0.1426]. For 71175 unique reflects, final R1[with $I > 2\sigma(I)$] = 0.1324, wR2 (all data) = 0.2349, GOOF = 1.010. CCDC NO. 2166181.

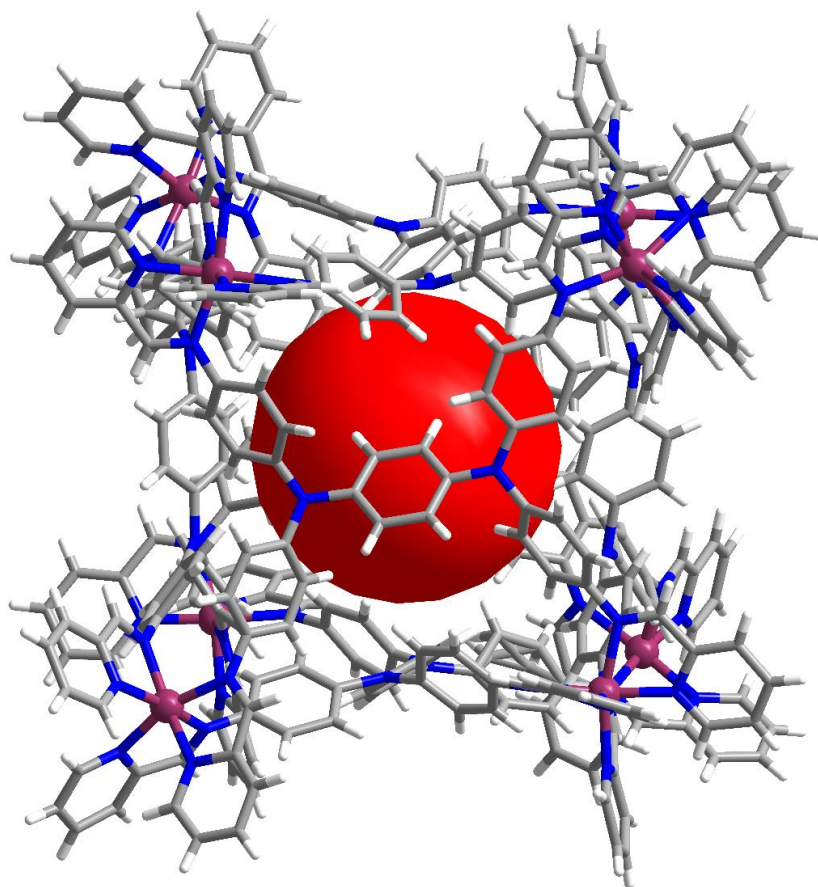


Figure S2. Structure of the cage **Zn-PAP** showing the coordination geometry of Zn ions and the potential pockets.

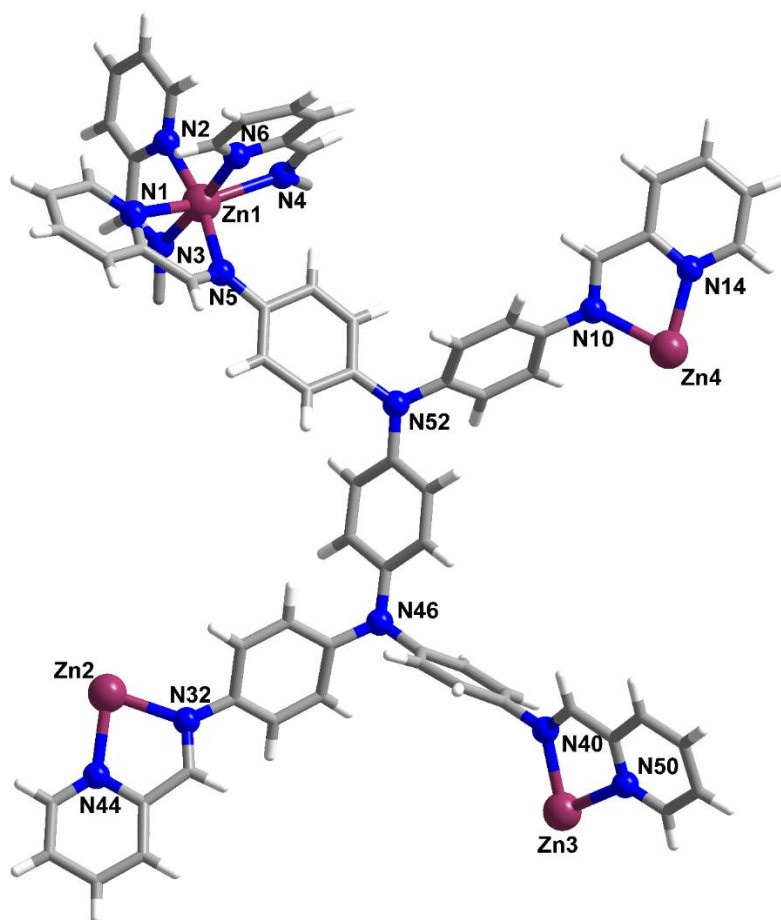


Figure S3. Molecular structure of the entire cage **Zn-PAP** is within a unique asymmetric unit, and the skeleton of only one ligand in **Zn-PAP** is shown for clarification, omitting the anion and solvent molecules.

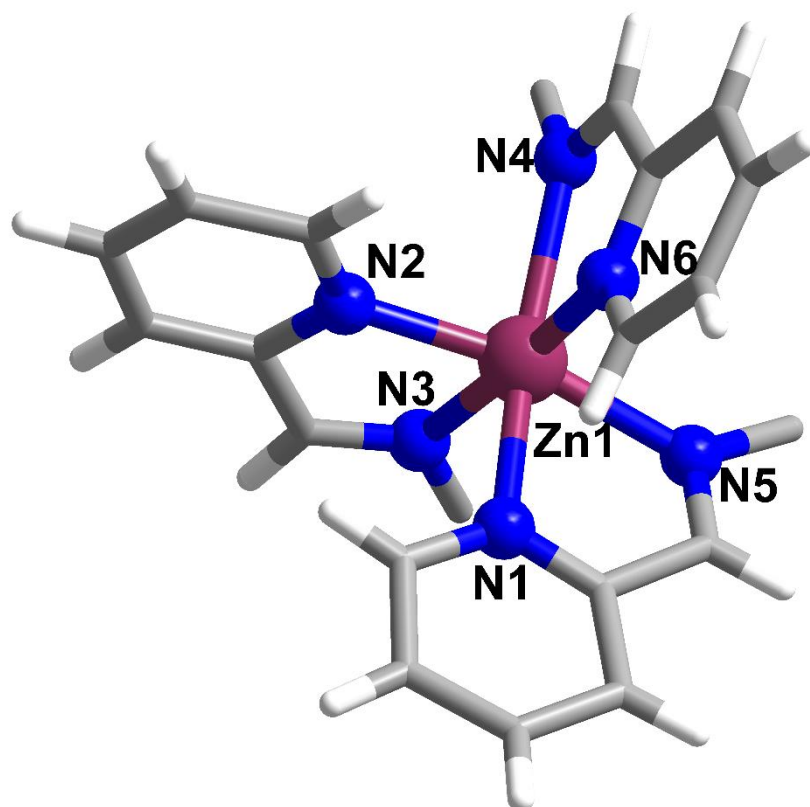


Figure S4. Coordination geometry of the Zn1 atom in cage **Zn-PAP**. Selected bond distances (Å) and angles (°). Zn1–N1 2.185(6), Zn1–N2 2.124(7), Zn1–N3 2.237(7), Zn1–N4 2.183(7), Zn1–N5 2.200(7), Zn1–N6 2.281(7), N2–Zn1–N4 97.5(3), N2–Zn1–N5 172.1(3), N2–Zn1–N6 100.6(3), N2–Zn1–N1 78.8(3), N2–Zn1–N3 97.0(3), N5–Zn1–N4 85.9(3), N5–Zn1–N3 76.0(3), N6–Zn1–N4 75.3(3), N6–Zn1–N5 87.1(3), N6–Zn1–N1 110.1(3), N6–Zn1–N3 156.2(3), N1–Zn1–N4 173.9(3), N1–Zn1–N5 97.1(2), N1–Zn1–N3 89.0(2), N3–Zn1–N4 86.6(3).

3. ESI-MS Spectra data

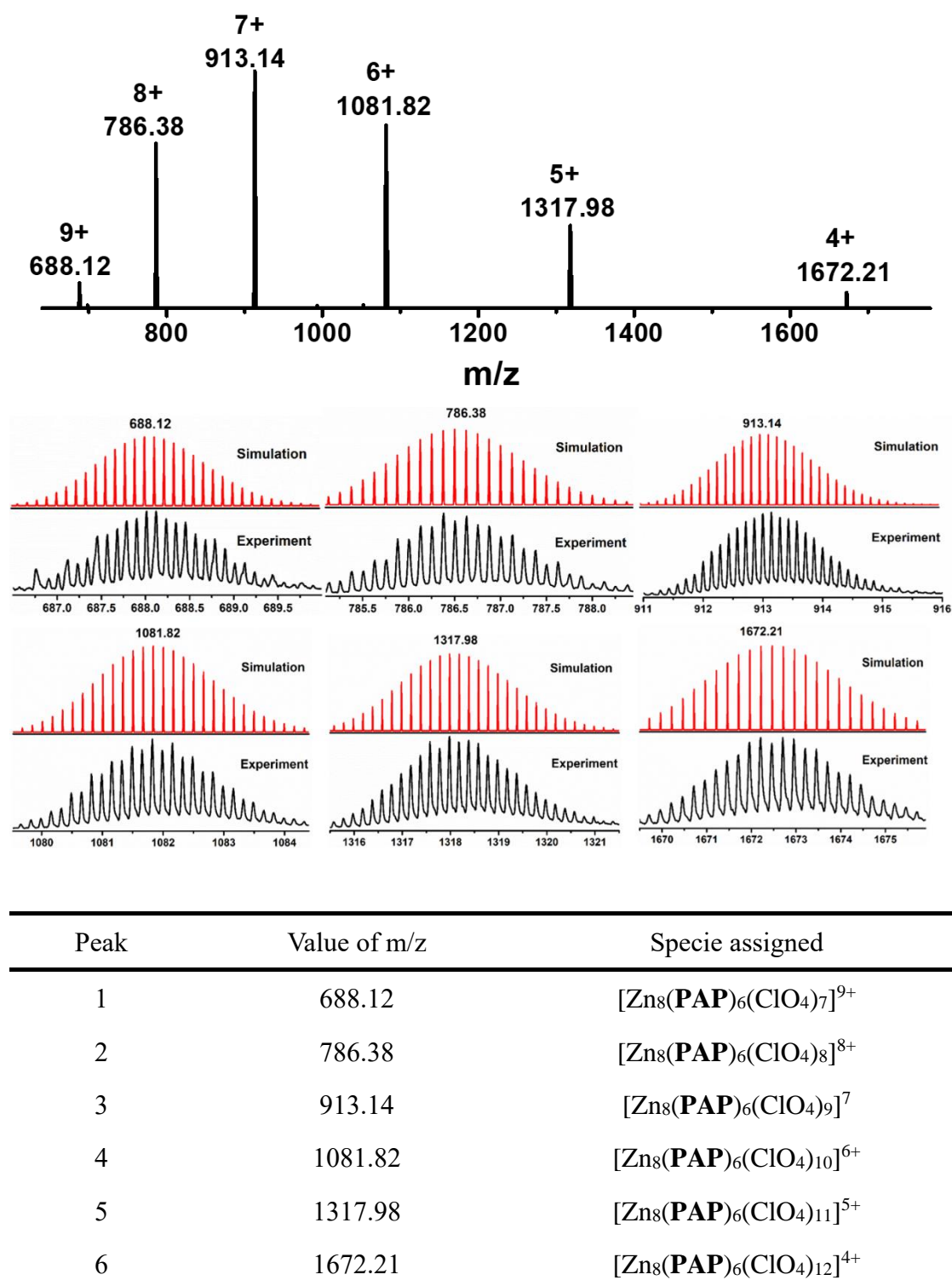
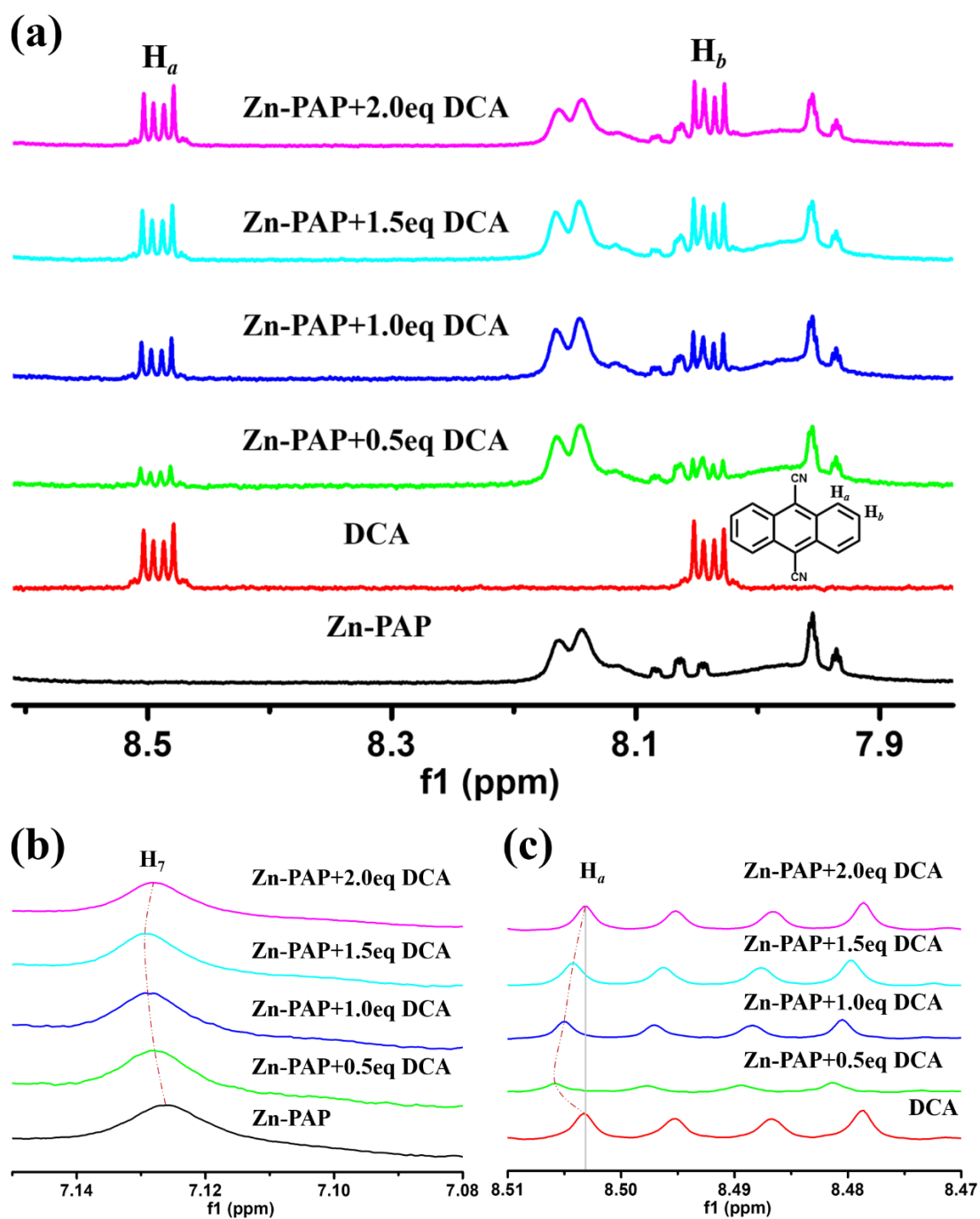


Figure S5. The ESI-MS spectrum of **Zn-PAP** (0.10 mM) in CH₃CN solution.

4. Characterization of Host-Guest

$^1\text{H-NMR}$ Spectra of the host-guest complexes



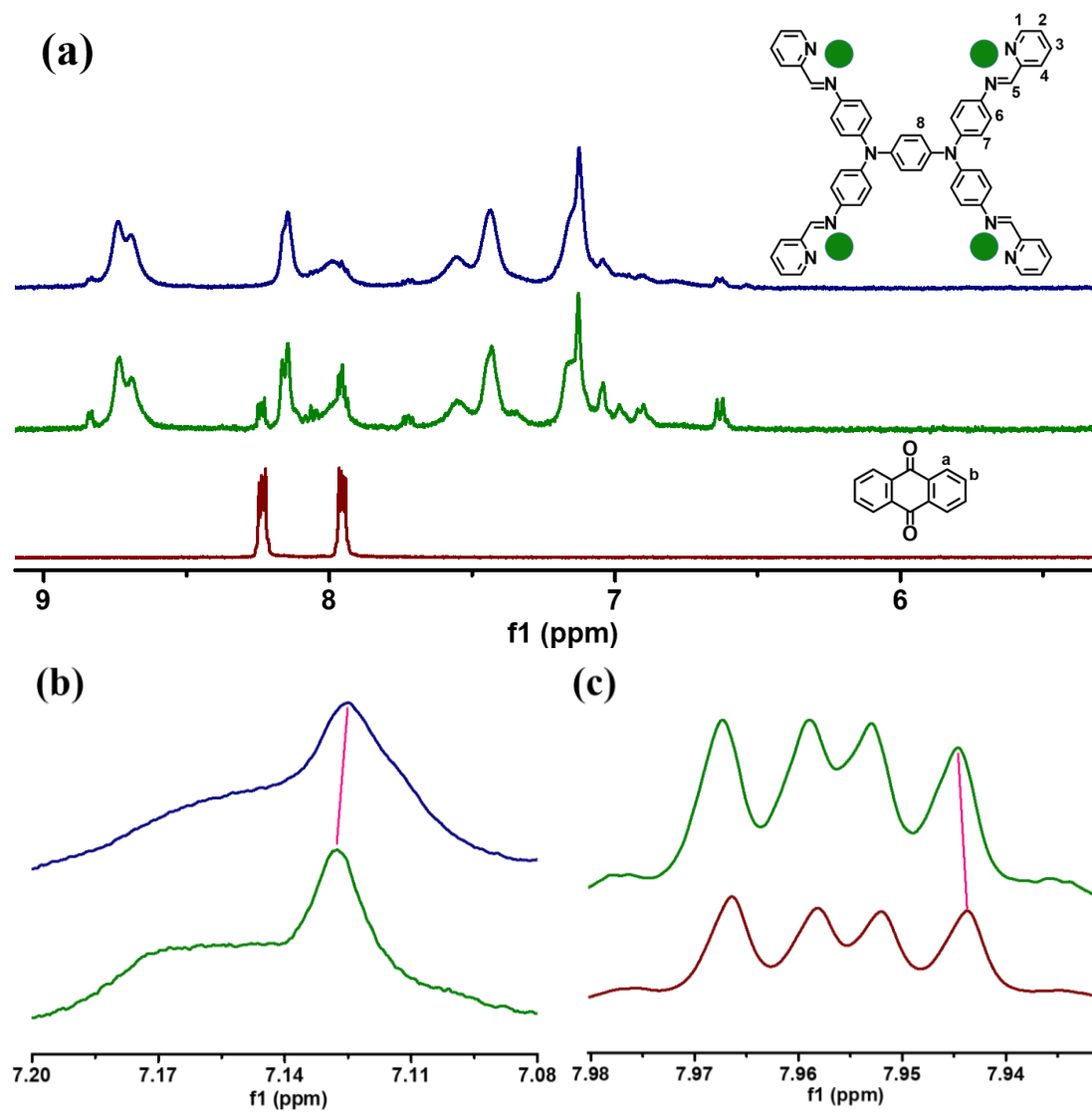


Figure S7. (a) ^1H -NMR spectrum of **Zn-PAP** (0.1 mM, blue line), **Zn-PAP** (0.1 mM) upon addition of **AQ** (0.1 mM, green line), and **AQ** (0.1 mM, red line) in d^6 -DMSO. (b) Uphill of the protons of **Zn-PAP** (H_7). (c) Downhill of the protons of substrate **AQ** (H_b).

Isothermal titration calorimetry

The ITC was performed on a Nano ITC (TA Instruments Inc.–Waters LLC) at atmospheric parameters and at 25.0 °C, giving the apparent dissociation constants and the thermodynamic parameters. The solution of guest in the syringe was sequentially injected under stirring at 250 rpm into a solution of host in the sample cell.

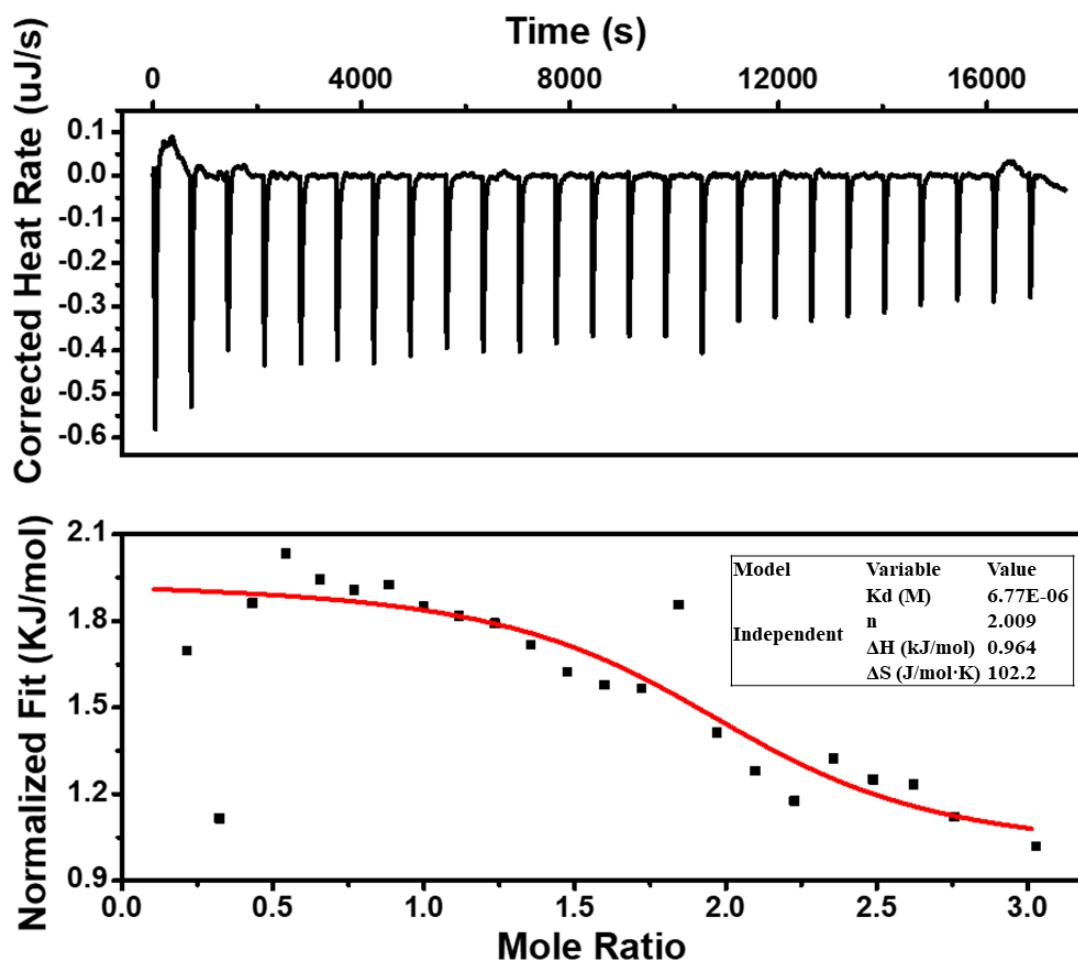


Figure S8. Microcalorimetric titration of **Zn-PAP** with guest **AQ** in DMAC solution at 298.15K. Raw data for sequential 25 injections (10 μ L per injection) of **AQ** solution (1.0 mM) injecting into **Zn-PAP** solution (0.1 mM). Apparent reaction heat obtained from the integration of calorimetric traces.

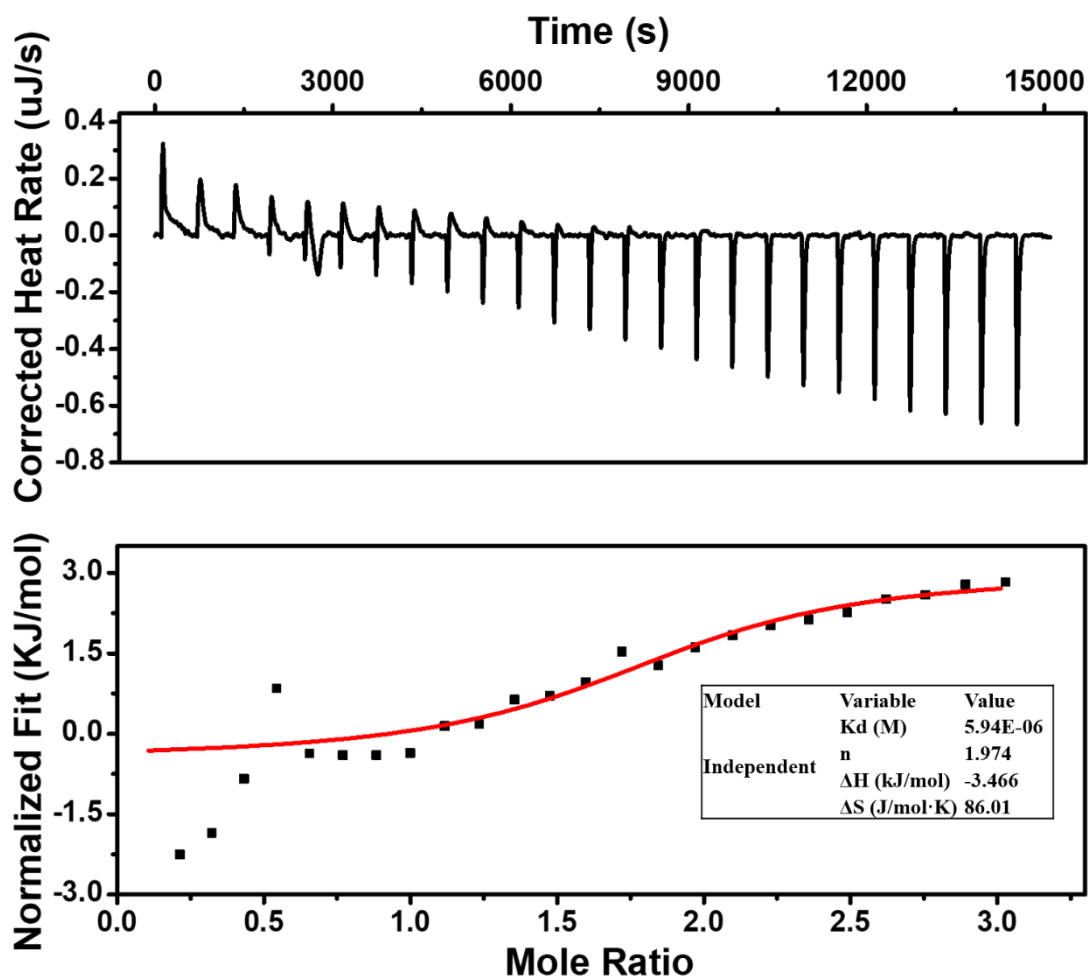


Figure S9. Microcalorimetric titration of **Zn-PAP** with guest **ATP** in DMAC solution at 298.15K. Raw data for sequential 25 injections (10 μ L per injection) of **ATP** solution (1.0 mM) injecting into **Zn-PAP** solution (0.1 mM). Apparent reaction heat obtained from the integration of calorimetric traces.

Fluorescence titration experiment

The solution fluorescence spectra were measured on Edinburgh FS920 steady-state fluorescence spectrophotometer. In a DMAC solution containing **DCA** (10 μM) (black line) upon addition of **L** (10 to 20 μM), the fluorescence intensity was recorded at 442 nm and 468 nm and excited at 395 nm.

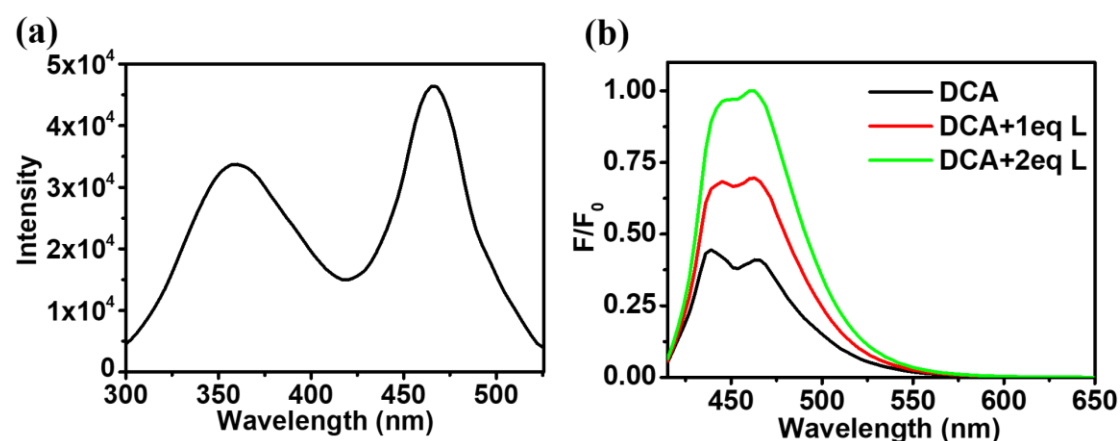


Figure S10. (a) Excitation spectra of **Zn-PAP** (10 μM) in DMAC, the fluorescence intensities were recorded at 360 nm and 460 nm with emission at 590 nm. (b) Emission spectra of **DCA**(10 μM , black line) in DMAC upon the addition of **L** (10 to 20 μM , colored lines), the fluorescence intensities were recorded at 442 nm and 468 nm and excited at 395 nm.

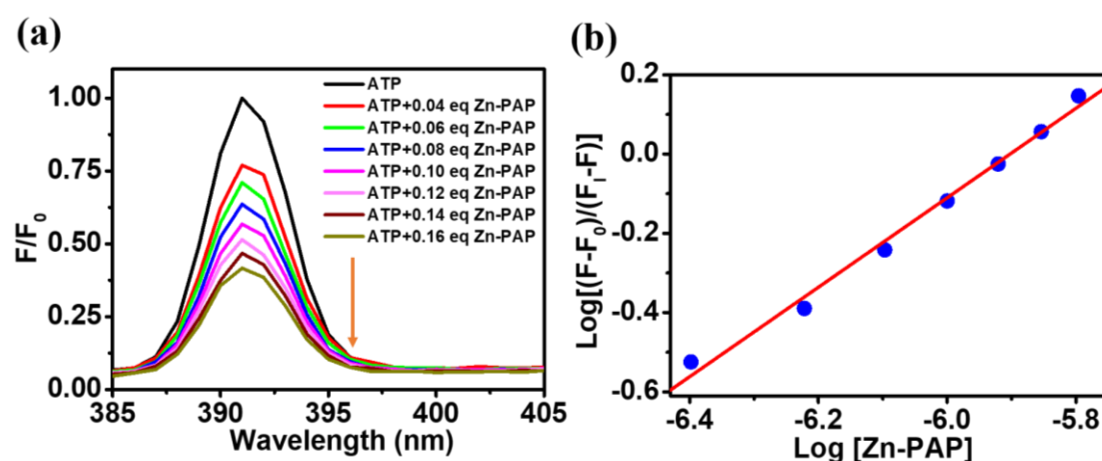


Figure S11. (a) Emission spectra of **ATP** (10 μM , black line) in DMAC upon the addition of **Zn-PAP** (0.4 to 1.6 μM , colored lines), the fluorescence intensities were recorded at 391 nm and excited at 351 nm. (b) The Hill plot of the titration curve of fluorescein upon the addition of **Zn-PAP**.

UV-vis titration experiment

The UV-vis spectra of solutions were performed on a SHIMADZU UV 2600 spectrophotometer. At the beginning of the UV titration experiment, the cage solution was added to both the reference and sample cells to deduct the background peaks of the cage. The differential UV spectra were obtained after subtracting the UV peaks of the guest.

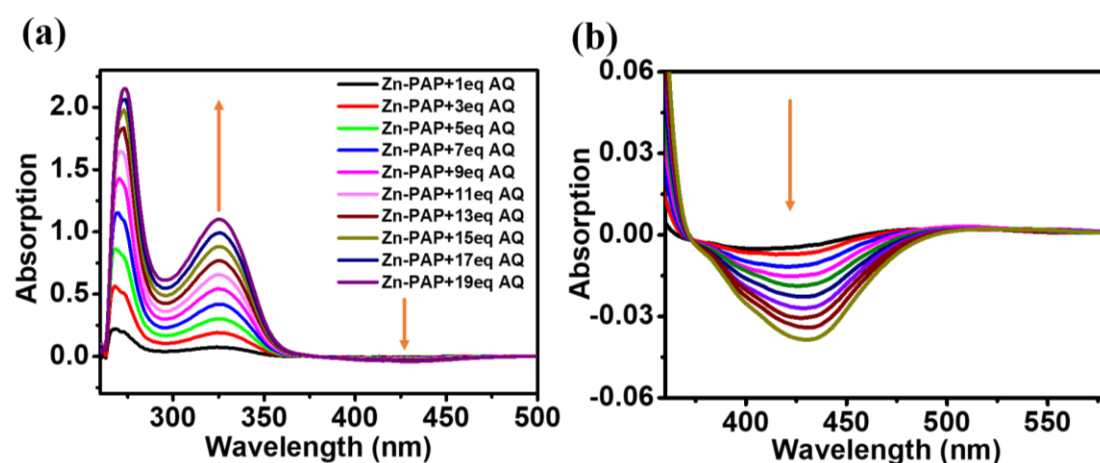


Figure S12. (a) Family of UV of **Zn-PAP** (10 μM) and **AQ** (10 to 190 μM) in DMAC showed the characteristic peaks of **AQ** at 273 nm and 327 nm. (b) Differential UV spectrum of **Zn-PAP** (10 μM) and **AQ**(10 to 190 μM) in DMAC after deducting the UV peaks of the guest **AQ**. The presence of isosbestic point at 430 nm indicated the host-guest behavior between **Zn-PAP** and **AQ**.

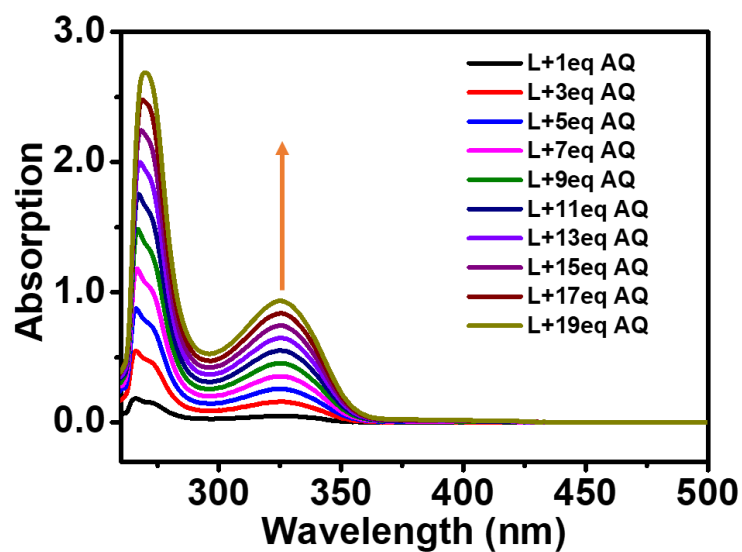


Figure S13. Family of UV of **L** (10 μ M) and **AQ** (200 μ M) in DMAC at the same conditions.

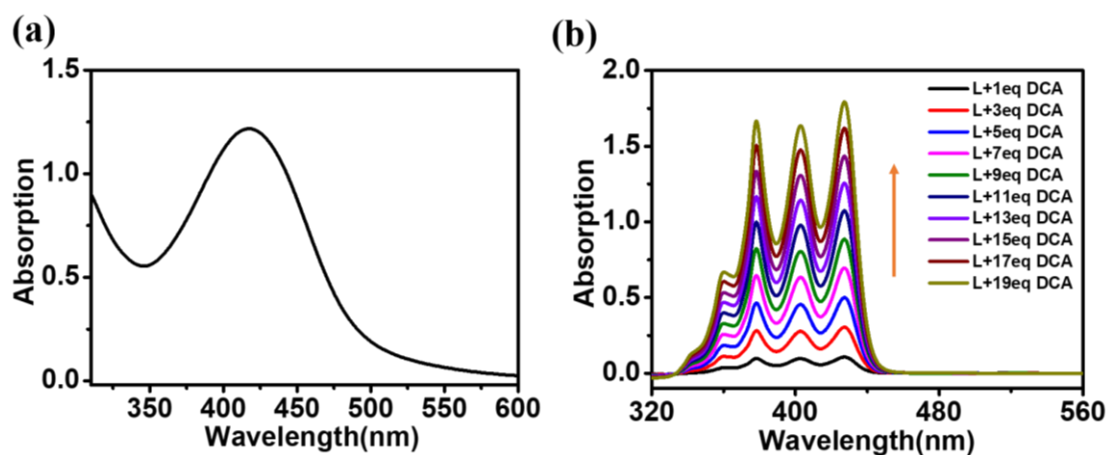


Figure S14. (a) UV spectrum of **Zn-PAP** (10 μ M) showed the characteristic peaks of **Zn-PAP** at 420 nm. (b) Family of UV of **L** (10 μ M) and **DCA** (200 μ M) in DMAC only showed the characteristic peaks of **DCA** at 378 nm, 402 nm, and 428 nm.

Electrochemical experiment

The electrochemical measurements were performed on a CHI 660E electrochemical workstation with a three-electrode system, with Ag/AgCl electrode as reference electrode, platinum silk as counter electrode, and glassy carbon electrode as working electrode, and. The measurements were made after degassing the solutions with argon to eliminate the effects of oxygen. The cyclic voltammetry of **Zn-PAP** was shown in DMAC solutions using 0.10 M (n-Bu₄N)⁺(PF₆)⁻ as the supporting electrolyte with the scan rate of 100 mV/s.

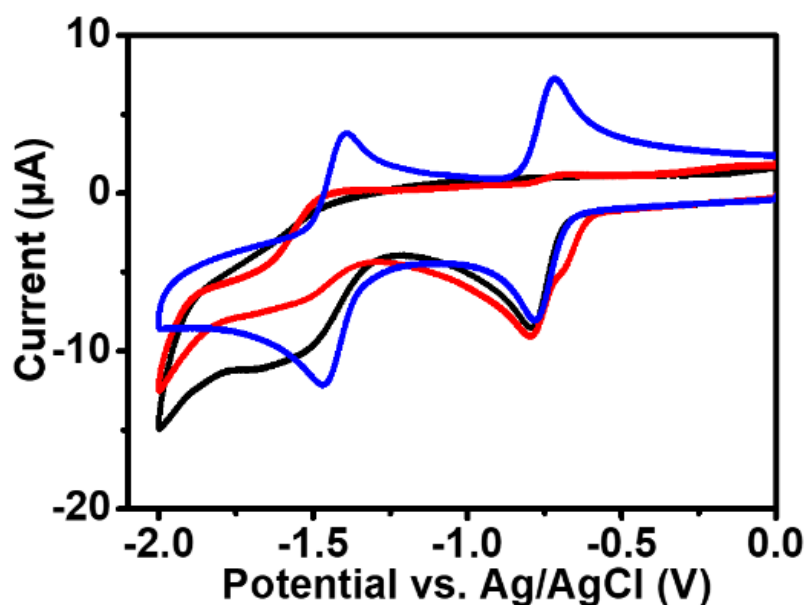


Figure S15. Cyclic voltammetry of **Zn-PAP** (0.10 mM) (black line), **AQ** (0.50 mM) (blue line), and **Zn-PAP** (0.10 mM) upon addition of **AQ** (0.10 mM) (red line).

5. Data for the photocatalytic reactions

In the photocatalytic reduction kinetics experiments with substrate 4-chlorobenzamide, the reaction progress was followed by extracting 100 μL of the reaction mixture each time with a long needle, followed by GC analysis after a quick silica gel wash. The product yield in the initial stage is taken as the initial rate of the reaction.

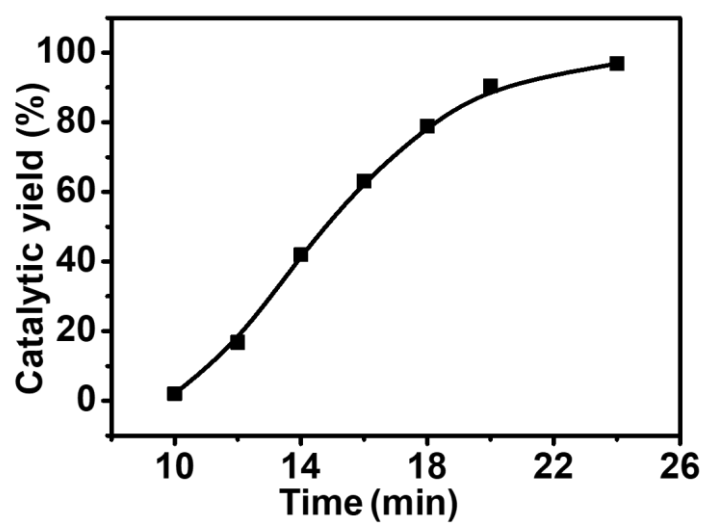


Figure S16. Kinetics of the product benzamide conversion under standard conditions.

GC data for the photocatalytic reactions

Peaks	Retention time (min)	Height	Area	Area (%)
10min				
1	4.967	193222	412252	69.929
2	8.363	346	3470	0.589
3	10.747	12485	173807	29.482
12min				
1	4.965	195931	414576	72.662
2	8.232	3031	27566	4.832
3	10.740	9579	128409	22.506
14min				
1	4.964	206509	430006	71.481
2	8.182	6766	80057	13.308
3	10.826	7583	91507	15.211
16min				
1	4.965	190474	403785	70.906
2	8.181	8399	109036	19.147
3	10.913	3249	47977	9.947
18min				
1	4.965	186447	399102	70.274
2	8.170	8941	131100	23.084
3	10.960	2761	28358	6.642
20min				
1	4.965	186073	399313	70.278
2	8.172	9890	143138	25.192
3	11.004	2240	19754	4.530
24min				
1	4.967	192740	411289	70.296
2	8.156	11355	158104	27.022
3	11.086	725	3922	2.682

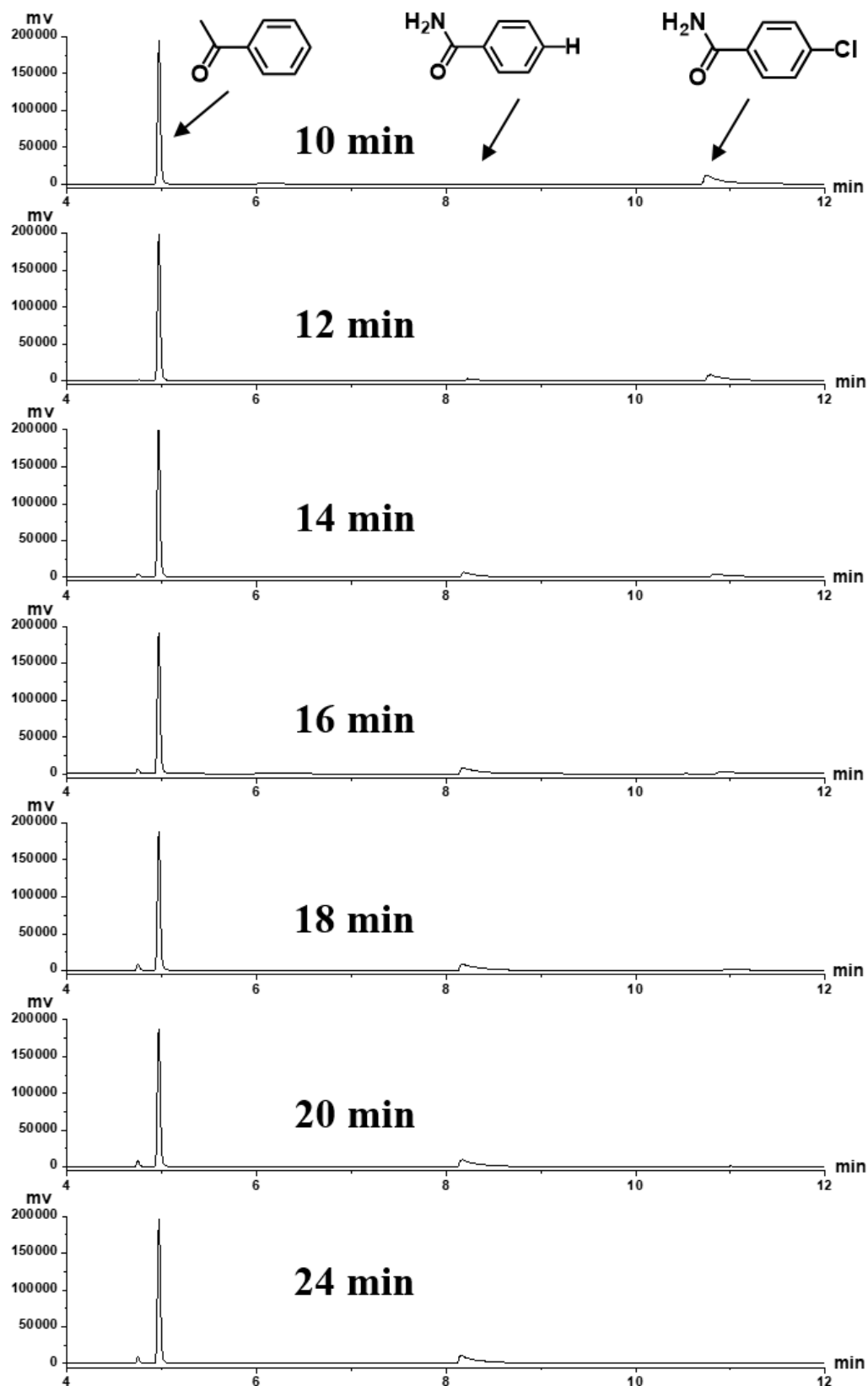


Figure S17. GC data for the yields of benzamide of the photocatalytic reduction of 4-chlorobenzamide catalyzed by **Zn-PAP** (0.5 μM) using acetophenone as integral standard at 10 min, 12 min, 14 min, 16 min, 18 min, 20 min, 24 min, respectively.

Cyclic catalysis experiment

Cyclic catalysis experiments were performed by adding one aliquot of 4-chlorobenzamide to react for 30 minutes before adding the next aliquot of 4-chlorobenzamide. The yields of each cyclic reaction were measured by GC analysis. The UV spectra of the solutions after each reaction were measured by aspirating 100 μL reaction solution and adding DMAC to prepare a 3 mL dilute solution.

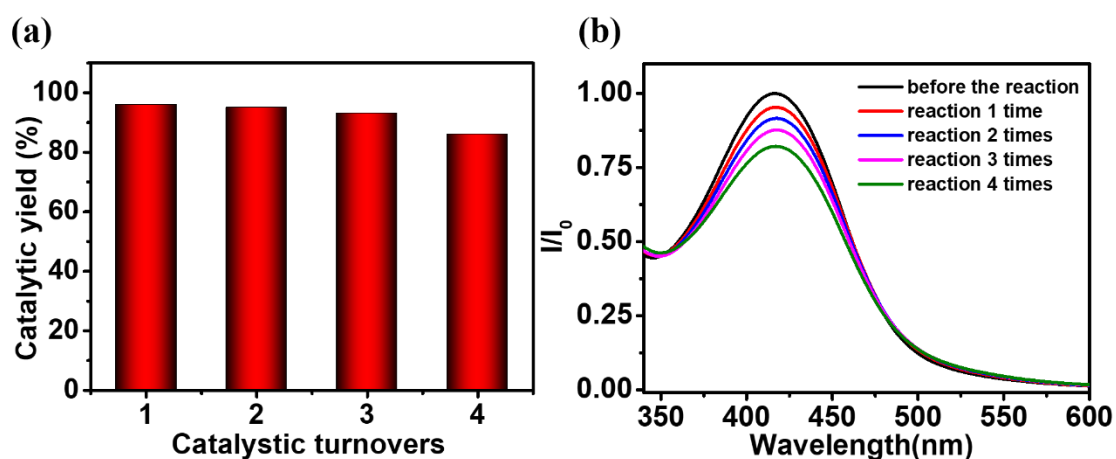


Figure S18. (a) Under standard catalytic reaction conditions, an aliquot of 4-chlorobenzamide was added after each 30 minutes of reaction under illumination to measure the yields. (b) The UV spectra of the reaction solutions before and after cyclic catalysis, showing that the characteristic peak of **Zn-PAP** at 420 nm slightly decreased with increasing number of cycles.

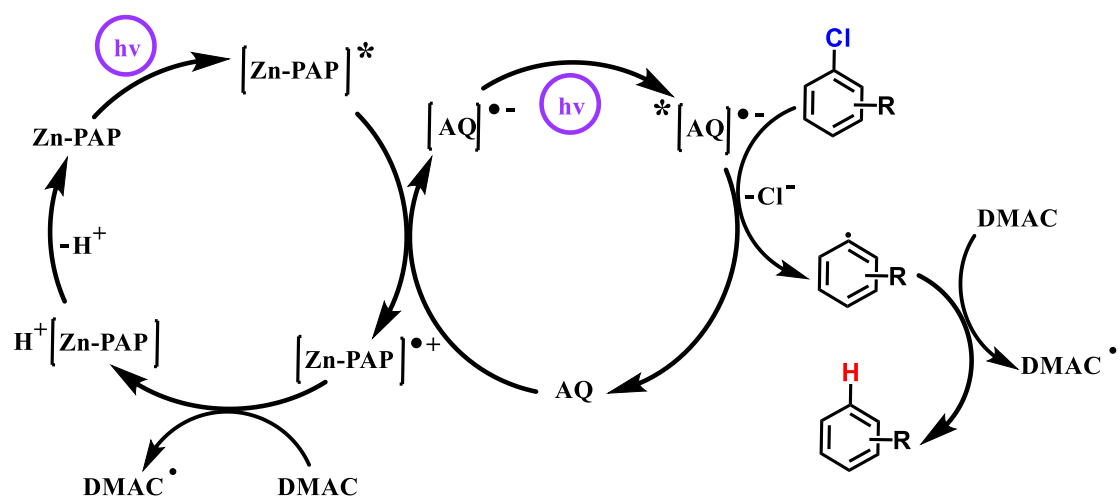


Figure S19. Possible mechanism of the photoredox catalytic cycle for the photoreduction of aryl chlorides.^{S5,S6}

6. References

- S1. SMART Data collection software (version 5.629); Bruker AXS Inc., Madison, WI, **2003**.
- S2. SAINT, Data reduction software (version 6.45); Bruker AXS Inc., Madison, WI, **2003**.
- S3. G. M. Sheldrick, *Acta Cryst. A* **2015**, 71, 3.
- S4. O. V. Dolomanov, L. J. Bourhis, R. J. Gildea, J. A. K. Howard, H. Puschmann, *J. Appl. Cryst.* **2009**, 42, 339.
- S5. L. Hou, X. Jing, H. Huang and C.-Y. Duan, *ACS Appl. Mater. Interfaces*, **2022**, 14, 15307-15316.
- S6. J. He, J. Li, Q. Han, C. Si, G. Niu, M. Li, J. Wang and J. Niu, *ACS Appl. Mater. Interfaces*, **2020**, 12, 2199-2206.